metals

MDPI

Article

Study on Shear Strength of Partially Connected Steel Plate Shear Wall

Yuqing Yang *, Zaigen Mu * and Boli Zhu

School of Civil and Resource Engineering, University of Science and Technology Beijing, Beijing 100083, China; zboly@ustb.edu.cn

* Correspondence: yqyang@ustb.edu.cn (Y.Y.); zgmu@ces.ustb.edu.cn (Z.M.)

Abstract: The paper proposes partially connected steel plate shear walls, in which the infill plates and frames are connected by discretely distributed fish plates at the corners and at the centers. The high lateral resistance of a steel plate shear wall has led to its widespread use in the design of structural shear resistance. In this paper, finite element models of the partially connected steel plate shear walls are established by the finite element method, and the effect of the different partial connections on the shear strength is firstly investigated. Moreover, the variation of the shear strength with the plate-to-frame connectivity ratio is analyzed numerically, and the effect of the connectivity ratio on the development of the tensile field is studied. Based on the numerical analysis results, the effect of the connectivity ratio on shear strength is evident at low levels. When the connectivity ratio is over 80%, the shear strength of the partially connected steel plate shear wall can reach 95% of that of the fully connected steel plate shear wall. When the connection ratio is at a low level, the advantages of the central connection on the shear strength of the structures are higher than those with corner connections. Furthermore, the fitting formula for the partially connected steel plate shear wall is obtained by changing the connectivity ratio and width-to-height ratio of the examples, which can predict the shear capacity of the partially connected steel plate shear wall with different partial connections.

Keywords: partially connected steel plate shear wall; shear strength; connectivity ratio; finite element method; design formula

check for updates

Citation: Yang, Y.; Mu, Z.; Zhu, B. Study on Shear Strength of Partially Connected Steel Plate Shear Wall. *Metals* **2022**, *12*, 1060. https://doi.org/10.3390/met12071060

Academic Editor: Denis Benasciutti

Received: 27 April 2022
Accepted: 15 June 2022
Published: 21 June 2022

Publisher's Note: MDPI stays neutral with regard to jurisdictional claims in published maps and institutional affiliations.

Copyright: © 2022 by the authors. Licensee MDPI, Basel, Switzerland. This article is an open access article distributed under the terms and conditions of the Creative Commons Attribution (CC BY) license (https://creativecommons.org/licenses/by/4.0/).

1. Introduction

The infill plate of steel plate shear wall (SPSW) structures is usually fully connected to the boundary elements by fish plates or bolts (Figure 1). The steel plate shear wall has high lateral resistance and energy dissipation capability [1], hence, it is a better choice for lateral resistant members of structures and is widely used in multi-rise and super-tall structures. In 1931, Wanger [2] studied the post-buckling strength of thin aluminum alloys and proposed the "Theory of pure diagonal tension". Then, Basler [3] considered uniform tensile stresses in the tensile field and presented the shear force of a thin steel web. In 1983, Thorburn et al. [4] applied the theory of tensile field to thin steel plate shear walls. Since then, many types of thin steel plate shear walls were developed, including unstiffened, stiffened, buckling-restrained, perforated, composited, low-yield-point steel or aluminum [5–10], and metal shear panels show good performance [11]. Among them, unstiffened steel plate shear walls are the most basic and common. The development of the tension field of the infill plate affects the bearing capacity of the structure. Therefore, the performance of the infill plate after buckling and the lateral resistance of the infill plate with different boundary conditions are the focus of the study.

Yu et al. [12] proposed a new connection type, allowing for reducing the requirement of bolt hole accuracy for traditional bolted connections. The infill plate is connected to boundary frames through angles steel, which can facilitate the installation and maintenance of steel plate shear walls. Paslar et al. [13] studied six different connection types of plate-to-frame connections and evaluated their structural performance by comparing them with

the fully connected plate, as shown in Figure 2. The infill plate connected to the columns reduces the bearing capacity more than the plate connected to the beams. When the ratio of plate-to-frame connection is above 80%, all lateral resistance properties can reach 95% of the full connection type, including lateral load capacity, ductility, and stiffness. Azandariani et al. [14] conducted a parametric analysis with a three-story steel plate shear wall and studied the base shear capacity of SPSWs with partial plate-to-column connections of different width-to-height (aspect) ratios and high-to-thickness ratios. The results show that partial plate-to-column connections can reduce the additional effect on the columns, but the stiffness and shear strength of the structure decreased by approximately 25% on average.

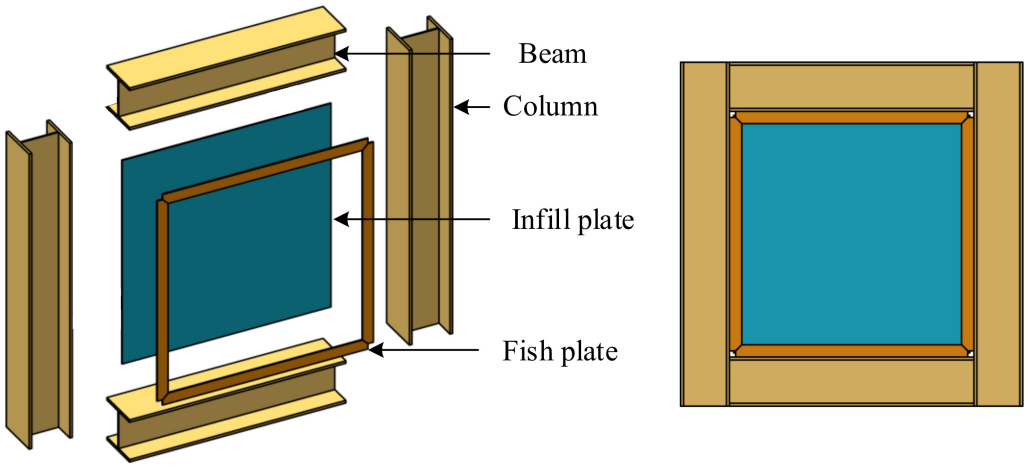


Figure 1. Steel plate shear wall.

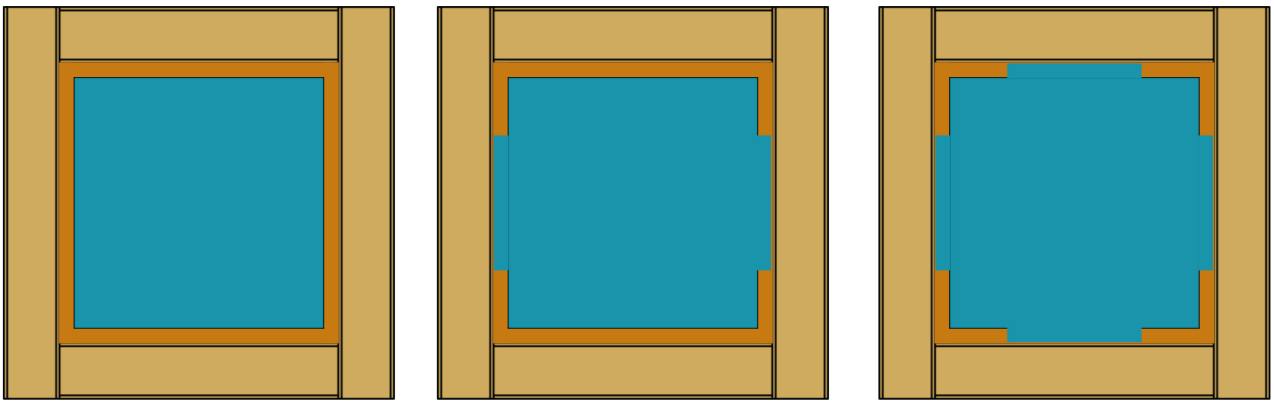


Figure 2. Steel plate shear wall with partial connection.

Wei et al. [15,16] proposed a buckling-restrained SPSW with four-corner connections, where the structure is only connected to the boundary frame at the four corners of the infill plate. Du et al. [17] proposed to partially connect the infill plate of the buckling-restrained SPSW to the concrete-filled steel tubular columns, including the four-corner connection and partial column connection. Mirsadeghi and Fanaie [18] investigated the effect of the plate-to-column connectivity ratio on structural performance. Through experiments and numerical calculations, when the ratio of the plate-to-frame connection exceeds 70%, the plate develops entire parallel tensile strips.

There are some papers that demonstrate that the finite element software ABAQUS [19] can simulate the shear behavior of the steel plate shear wall by using a reasonable set of material parameters and boundary conditions [20–22]. Moreover, numerical simulations are in good agreement with the experimental results and save time and the cost of tests [23]. Thus, finite element simulations can be used to predict the behavior of the structures.

Currently, the primary focus of existing research is a quantitative analysis of the overall behavior of the partially connected steel plate shear wall (PC-SPSW). However, the results of the investigation on the shear strength of the infill plate are less encouraging, and the bearing capacity calculation formulae that take the connectivity ratio into account are unavailable. This study proposes eight different types of PC-SPSW. The effect of connectivity ratios on the shear behavior of the infill plate is studied by the finite element (FE) method, and the calculation formula of structural shear strength is provided.

2. Theoretical Analysis and Finite Element Modeling

2.1. Shear Strength of Infill Plate

The shear strength results of the finite element model are compatible with the test results and the theoretical calculation formula Equation (1). The shear strength of a thin infill plate with width b, height h, and thickness t can be calculated by the following equations [24].

$$F_{\text{plate}} = bt\tau_{\text{cr}} + \frac{1}{2}bt\sigma_t \sin(2\theta) \tag{1}$$

$$\begin{cases} \tau_{\text{cr}} = \frac{K\pi^2 E}{12(1-\nu)^2}\left(\frac{t}{b}\right)^2 \\ \sigma_t = -\frac{3}{2}\tau_{\text{cr}} \sin 2\theta + \sqrt{\sigma_y^2 + \left(\frac{9}{4}\sin^2 2\theta - 3\right)\tau_{cr}^2} \end{cases} \tag{2}$$

where τ_{cr} is the elastic buckling shear stress; σ_t is field tensile stress; σ_y is yield stress of steel plate; θ is the tension field inclination with respect to the vertical axis, which generally can be simplified to take 45°; K is the elastic buckling coefficient and can be calculated by the following formula when the four edges of the plate are simply supported [25]; ν is the Poisson's ratio, which is taken as 0.3.

$$\begin{cases} K = 5.35 + 4\left(\frac{b}{h}\right)^2 & \frac{b}{h} \geq 1 \\ K = 4 + 5.35\left(\frac{b}{h}\right)^2 & \frac{b}{h} < 1 \end{cases} \tag{3}$$

The specification [26] ignores the elastic buckling load of the infill plate, thus field tensile stress σ_t can be taken as the yield stress σ_y. Thus, the theoretical value of the shear strength of the infill plate can be calculated by Equation (4).

$$F_{\text{plate}} = \frac{1}{2}bt\sigma_y \sin(2\theta) \tag{4}$$

The beam-only connected steel plate shear wall can be seen as a type of PC-SPSW with a connectivity ratio of 0 to the column, as shown in Figure 3a. Ozcelik and Clayton [27] propose a method for calculating the base shear of the steel plate shear wall with a beam-connected web plate, as shown in Equations (5)–(7).

$$F_{\text{plate}} = \frac{1}{2}\left(1 - \frac{\tan\theta}{b/h}\right)bt\sigma_y \sin(2\theta) \tag{5}$$

$$\theta = \eta \tan^{-1}\left(\frac{b}{h}\right) \tag{6}$$

$$\eta = 0.55 - 0.03\left(\frac{b}{h}\right) \geq 0.51 \tag{7}$$

The shear strength of the steel plate shear wall which is partially connected to columns from two corners can be calculated using Equation (8) [18]. Where h_{nc} is not connected to a length of the plate in Figure 3b.

$$F_{\text{plate}} = \frac{1}{2}(1 - h_{nc}\tan\theta)bt\sigma_y \sin(2\theta) \tag{8}$$

Wei et al. [15] assume the diagonal formation of tension and compression fields, illustrated in Figure 3c and equivalent tension and compression strips are used to calculate the shear strength of the structure. By comparing Equations (4), (5), and (8), it can be seen that the shear strength of PC-SPSW is related to the fully connected steel plate shear walls with the connectivity ratio γ, such as Equation (9).

$$F = [1 - f(\gamma)]F_{\text{plate}} = [1 - f(\gamma)]\frac{1}{2}\sigma_y bt \sin(2\theta) \quad (9)$$

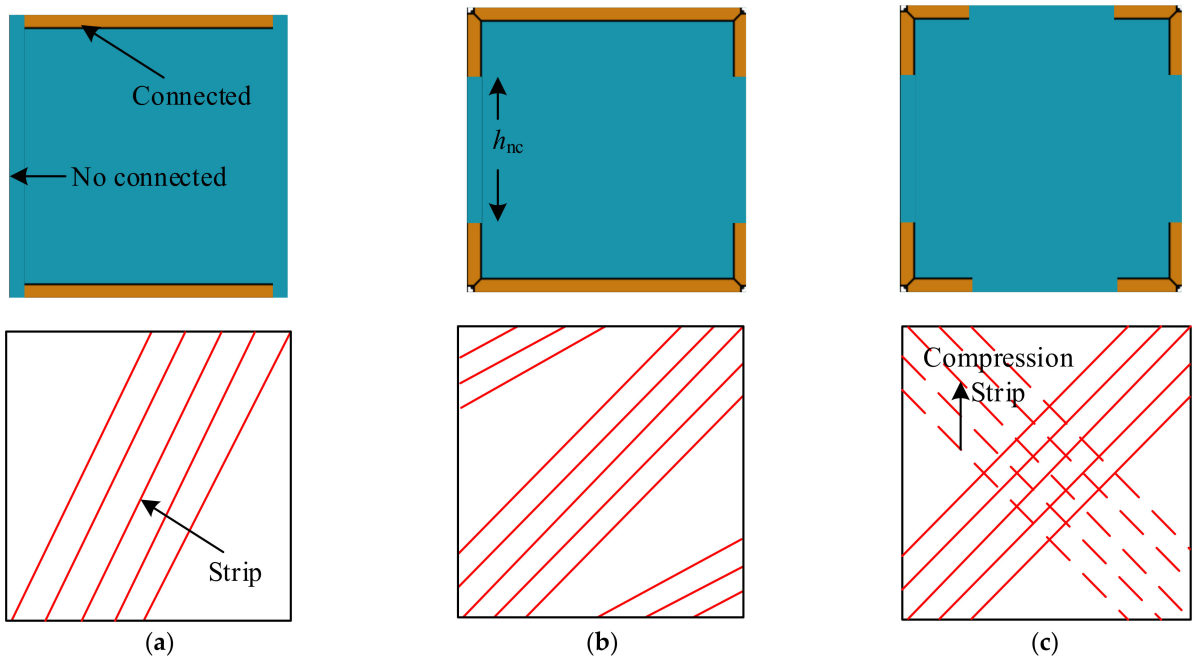


Figure 3. Simplified mechanical model for PC-SPSW: (**a**) Only beam connection; (**b**) Partially column connection; (**c**) Four-corner connection.

2.2. Basic Model

First, a base model of SPSW with the pin-connected frame was established to study the shear capacity of the infill plate, and the results of the finite element model were compared with the theoretical equation of shear strength to verify the feasibility of the finite element model practicality.

Table 1 lists the parameters of the steel plate shear wall model. The sections of the beams and columns are H750 mm × 600 mm × 18 mm × 36 mm and H600 mm × 600 mm × 18 mm × 36 mm, respectively, ensuring that the frame has enough rigidity to allow the steel plate material properties can be fully developed. The connection type of beam-to-column is pin linked. As a result, the influence of bearing capacity from the frame is eliminated.

Table 1. Parameters of SPSW model (Unit: mm).

Section of Column	Section of Beam	*h* of Plate	*b* of Plate	*t* of Plate
H600 mm × 600 mm × 18 mm × 36 mm	H750 mm × 600 mm × 18 mm × 36 mm	3000	3000	10

A base model of the steel plate shear wall is established in ABAQUS 6.13 developed by Dassault Systèmes, Waltham, MA, USA [19]. The beams and columns use beam element B31. The infill plate uses shell element S4R, which is suitable for thin panels with hourglass control [28]. The thickness direction of the plate uses the Simpson integral with a thickness integration point of 5. The beam-column connection is a PIN connection by MPC constraint, and the infill plate-to-frame connection is simulated by a TIE connection. The effect of fish

plates and residual stresses of the infill plate is not considered. The yield stresses of the frame and the infill plate are 345 MPa and 240 MPa, respectively. The elastic modulus E of steel is 206,000 MPa and von Mises criterion is used as the yield criterion.

2.3. Nonlinear Analysis

Steel plate shear walls deform in buckling before yielding, forming a tension field to resist the shear forces. As the tension field develops, the out-of-plane deformation increases. The structure reaches its ultimate state when the plate yields the material. Therefore, considering the geometric and material nonlinearities can accurately determine the shear capacity of the structure [29].

Furthermore, steel plates are not ideal flat plates and have initial defects due to manufacturing, transportation and installation. Initial imperfections can be obtained in three ways: the first is to actually measure the initial deformation of the plate; the second is to use trigonometric stochastic theory to describe the deformation distribution; and the third is to use the first-order buckling mode as the distribution model, assuming that the initial imperfections are distributed according to the most unfavorable distribution. The thin plate is very susceptible to buckling, and the amplitude of the initial imperfection does not have a significant effect on the analysis results [30]. Thus, the first-order buckling mode of the infill plate is used to approximate the distribution mode of the initial imperfection with a maximum geometric imperfection amplitude of $b/1000$ [30].

The influence of different mesh sizes on the structure was analyzed, as shown in Figure 4. When the mesh size was taken to be 400 mm or even less, the finite element results were in error with the theoretical values by less than 5%. The ratio of FE results to the theoretical value is basically 1 when 25 mm is taken, but it takes much time. Therefore, we ended up with a mesh size of 100 mm to minimize computational time while maintaining computational accuracy. The S4R element has no thickness, therefore, the mesh size of the model is 100 mm (length) × 100 mm (width).

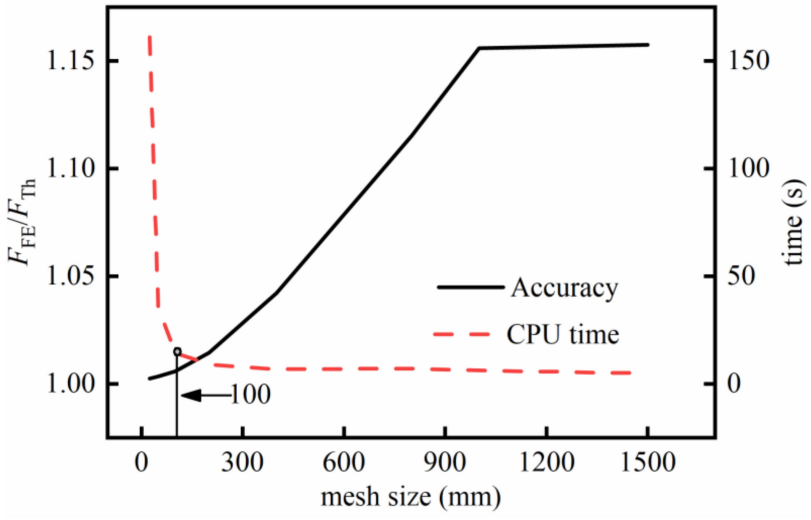


Figure 4. Curves of mesh size versus calculation accuracy and time.

The buckling analysis uses the subspace iterative method by ABAQUS/Buckle, the results are shown in Figure 5a. Then, the static analysis is solved by Newton's iterative algorithm in ABAQUS/Standard with considering geometric nonlinearity. In addition, material nonlinearity is considered and the stress–strain relationship of steel is an ideal elastic–plastic model without strain hardening, as shown in Figure 5b. The horizontal displacement is applied to the top beam to simulate the structure under shear load action and the maximum drift angle is 3%.

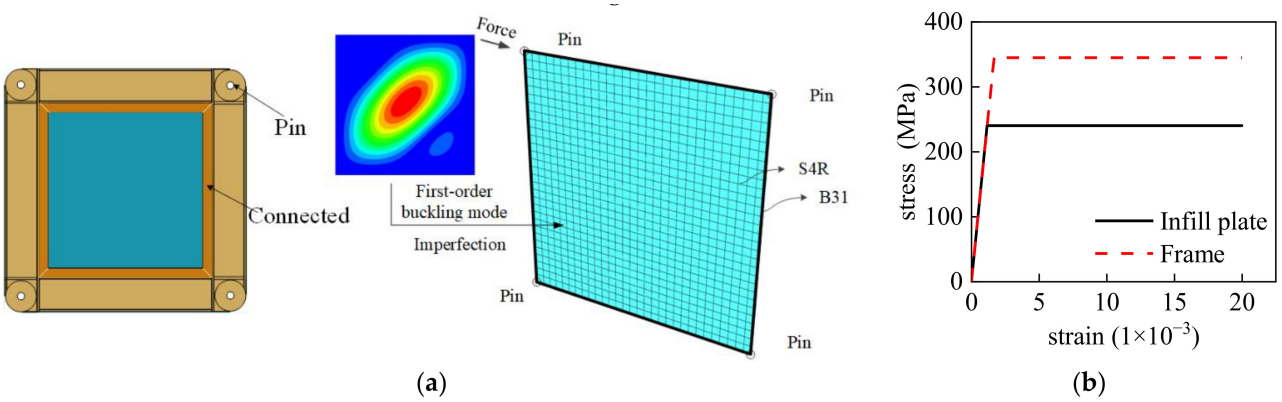


Figure 5. Finite element model of SPSW: (**a**) FE model of steel plate shear wall; (**b**) stress–strain relationship.

2.4. Verifying of FE Model

Figure 6 shows the load–displacement curve, von Mises stress, and plastic strain distribution of the SPSW model. At point A, the structure reaches the maximum bearing capacity and the infill plate has fully yielded. Then, with the horizontal displacement continuing to increase, the bearing capacity remains basically unchanged. The steel is assumed to be an ideal elastoplastic material without considering the hardening and failure of the material, so the ultimate bearing capacity of the structure at point B is equal to the theoretical shear strength of the infill plate. It should be noted that although the stresses in the plate all reach the yield stress of 240 MPa in Figure 6c, the plastic strain of the plate is not uniform and the strain changes along the diagonal direction are large, as can be seen in Figure 6d. The theoretical shear strength of the infill plate from Equation (4) is 3600 kN, and the ultimate bearing capacity obtained from the finite element model is 3623 kN. Varying the model parameters, the finite element results match the theoretical equation values, which can indicate the feasibility of the modeling and can be used for the subsequent analysis.

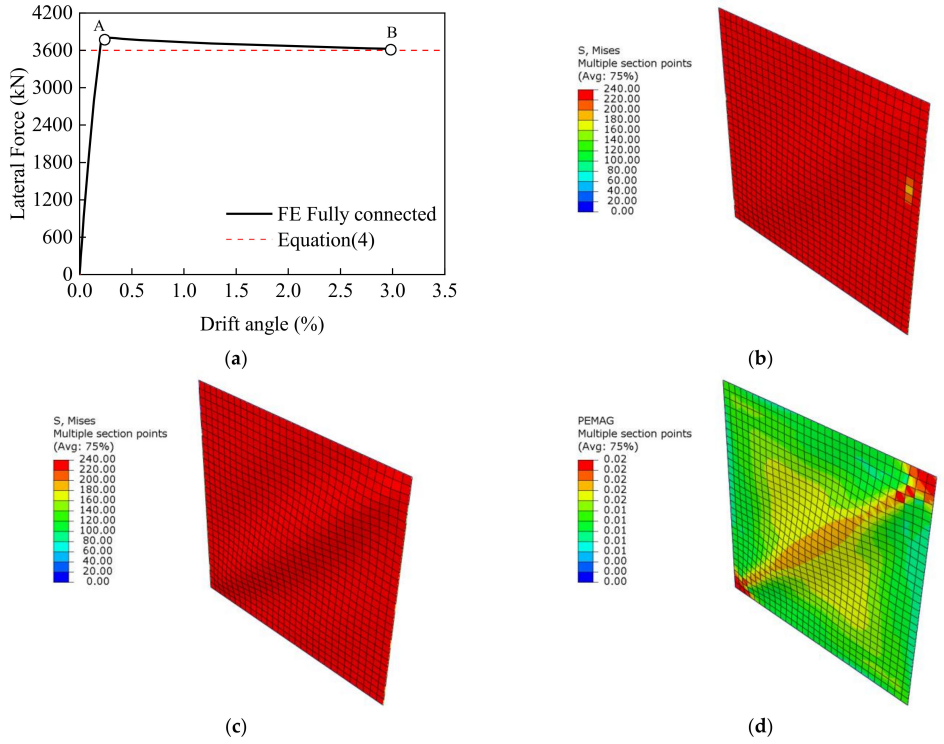


Figure 6. Load–displacement curve and stress of SPSW: (**a**) Load–displacement curve; (**b**) Stress distribution at point A; (**c**) Stress distribution at point B; (**d**) Plastic strain distribution at point B.

2.5. Description of Partial Connections

Based on the above model, eight different types of plate-to-frame connections are proposed, as shown in Figure 7. S1 is the plate that is completely attached to the beams, however, it is partially connected to columns from the center. S1R differs from the S1 in that it is partially connected to columns from two corners, with each connection segment being the same length. S2 is connected to a column in two segments, as opposed to S1, which has a one-segment connection. S3 and S4 plates are partially connected to both beams and columns in the same connection types.

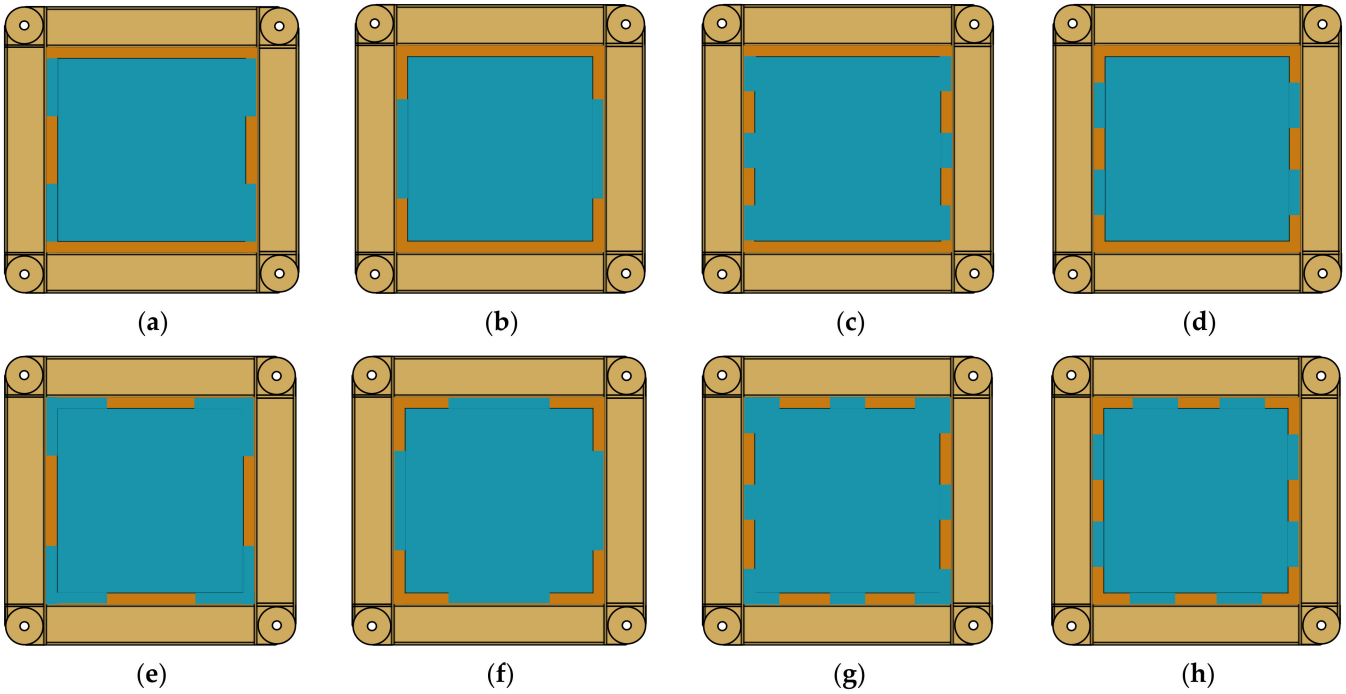


Figure 7. Different types of infill plate-to-frame connection: (**a**) S1; (**b**) S1R; (**c**) S2; (**d**) S2R; (**e**) S3; (**f**) S3R; (**g**) S4; (**h**) S4R.

The ratio of the attached length of the plate to the full length of the plate is defined as the plate-to-frame connectivity ratio, abbreviated as connectivity ratio γ. Table 2 list the models with different connectivity ratios. For instance, the S1-P13 model indicates that the S1 connection form with a connectivity ratio of about 13%; the S2-P100 means that the S2 connection form and the plate are fully connected to the columns.

Table 2. Models with different connectivity ratios.

Model	Connectivity Ratio γ of S1, S1R (%)	Connectivity Ratio γ of S3, S3R (%)	Model	Connectivity Ratio γ of S2, S2R (%)	Connectivity Ratio γ of S4, S4R (%)
P0	0 (Beamonly)	-	P0	0 (Beamonly)	-
P13	13	13	P20	20	20
P27	27	27	P40	40	40
P40	40	40	P60	60	60
P53	53	53	P80	80	80
P67	67	67	P100	100 (full)	100 (full)
P80	80	80	-	-	-
P93	93	93	-	-	-
P100	100 (full)	100 (full)	-	-	-

3. Numerical Results

3.1. Structural Performance of S1 and S1R Models

S1 and S1R are both fully connected to the beams, but different from the connection to the columns. The results of the shear strength of S1 and S1R are shown in Table 3, and the relationship between shear strength and the connectivity ratio is shown in Figure 8. The connectivity ratio can obviously affect the bearing capacity of steel plate shear wall structures. When the connectivity ratio is 0, S1 and S1R are beam-only connected, and the strengths of the models are approximately 53% reduced to that of the full connection model. Although the beam-only type can avoid the influence of the tension field on the columns, it also loses nearly half of the shear strength. In this way, the material properties of the infill plate cannot be fully developed. With an increase in the connectivity ratio, the strength of the structures gradually increases and approaches the shear strength of the fully connected plate. At the same connectivity ratio, the strength of S1 is higher than that of S1R.

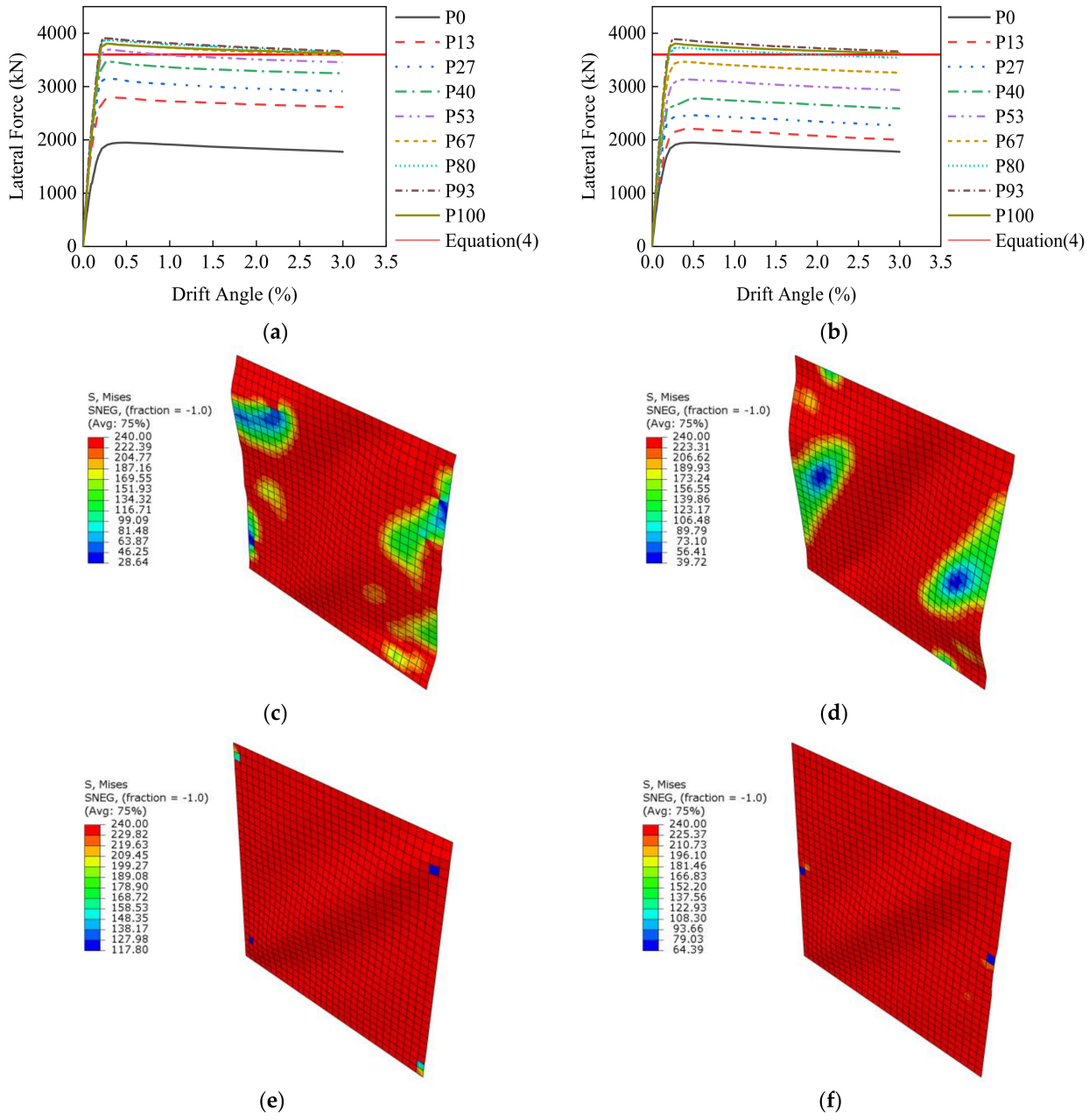


Figure 8. Load-displacement curves and stress distributions at 3% drift of S1 and S1R models: (**a**) S1; (**b**) S1R; (**c**) S1-P13; (**d**) S1R-P13; (**e**) S1-P80; (**f**) S1R-P80.

Table 3. Results of shear strength for S1 and S1R models.

Model	Connectivity Ratio γ (%)	S1		S1R	
		Value (kN)	Decrease Ratio (%)	Value (kN)	Decrease Ratio (%)
P0	0 (Beamonly)	1726	−52.91	1726	−52.91
P13	13	2615	−28.66	1997	−45.52
P27	27	2910	−20.62	2270	−38.07
P40	40	3251	−11.32	2589	−29.37
P53	53	3457	−5.70	2935	−19.94
P67	67	3585	−2.20	3259	−11.10
P80	80	3643	−0.62	3542	−3.38
P93	93	3665	−0.02	3660	−0.16
P100	100 (full)	3666	0	3666	0

From the stress diagram in Figure 8, when the connectivity ratio is small, the S1-P13 and S1R-P13 have a large area of the plate that does not reach the yield stress, of which S1R is larger. The steel cannot fully yield resulting in low bearing capacity. The development of the tension field was seriously affected in the unattached part due to the lack of anchorage from boundary elements. This effect decreases with an increase in connectivity ratio. The shear strength of the S1-P67, for which the connectivity ratio is 67%, almost reaches the full connection. For S1R, the shear strength of which almost reaches the fully connected type is the S1R-P80 model. When the beam is fully connected, increasing the connectivity ratio from the center can improve ultimate bearing capacity more than that from the corners.

3.2. Structural Performance of S2 and S2R Models

S2 is fully connected to the beams, but the center of the infill plate is partially connected to the columns in two segments. S2R is partially connected to the columns from the center and two corners. The ultimate bearing capacity results of S2 and S2R are shown in Table 4. The shear strength of S2 is higher than that of S2R with the same connectivity ratio. The shear strength of the S2 and S2R model gradually increases with an increase in the connectivity ratio. The shear strength of the S2 type with a connection ratio of 60% is close to the strength of the fully connected model. While the S2R-type requires a connection ratio of 80% for its shear strength to be approximately equal to the fully connected case. From Figure 9c,d at the connection of 20%, S2 and S2R extend a local low-stress region around the unconnected part and the area of the low-stress region of S2R is larger than that of S2. When the connection rate reaches 80%, in Figure 9e,f the steel plates of S2 and S2R are basically all in the plastic state.

Table 4. Results of shear strength for S2 and S2R models.

Model	Connectivity Ratio γ (%)	S2		S2R	
		Value (kN)	Decrease Ratio (%)	Value (kN)	Decrease Ratio (%)
P0	0 (Beamonly)	1776	−51.55	1776	−51.55
P20	20	2986	−18.54	2513	−31.45
P40	40	3356	−8.45	2985	−18.57
P60	60	3579	−2.37	3394	−7.41
P80	80	3652	−0.38	3626	−1.09
P100	100 (full)	3666	0	3666	0

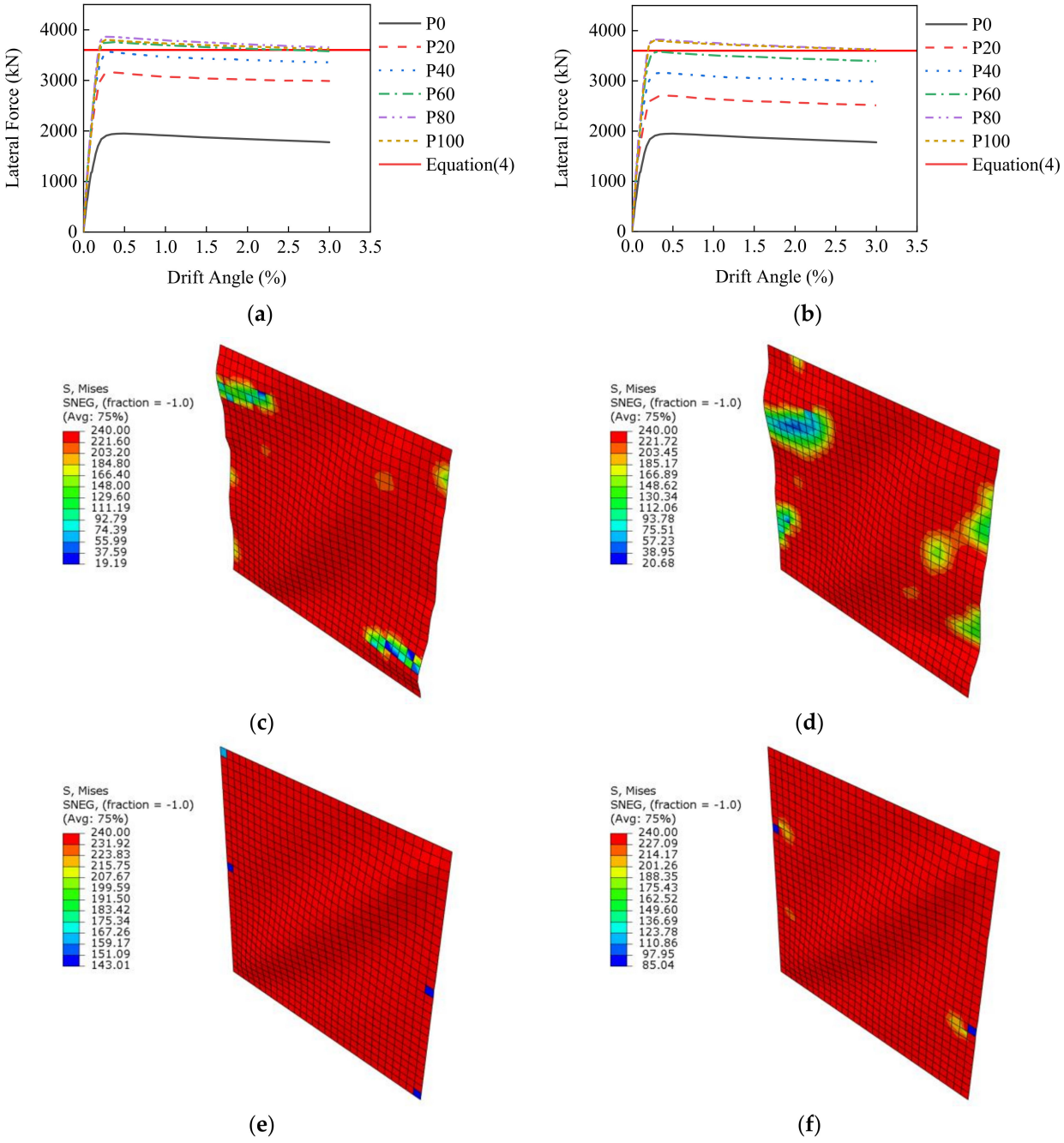


Figure 9. Load–displacement curves and stress distributions at 3% drift of S2 and S2R models: (**a**) S2; (**b**) S2R; (**c**) S2-P20; (**d**) S2R-P20; (**e**) S2-P80; (**f**) S2R-P80.

3.3. Structural Performance of S3 and S3R Models

The plate of S3 is connected to beams and columns from the centers, while S3R is connected from the corners. Table 5 displays the shear strengths of S3 and S3R. S3 and S3R have comparable shear capacities. The shear strength of the S3-P80 is almost as high as the full connection model, but the S3R-P80 has approximately 8% less strength. The stress distribution of the two types is obviously not the same in Figure 10c,d. S3-P13 has a visible tension field in the middle of the infill plate. The middle of the plate is yielded, whereas the unattached edge of the four corners has a large area in low stress. There is a large area of unyielding in the middle of the S3R-P13, where the yield area is applied only at the four corners without a tension field. When the connection ratio reaches 80, the plates of S3 and S3R almost yield, and both have an obvious tension field in Figure 10e,f.

Table 5. Results of shear strength for S3 and S3R models.

Model	Connection Ratio γ (%)	S3		S3R	
		Value (kN)	Decrease Ratio (%)	Value (kN)	Decrease Ratio (%)
P0	Not connected	0	−100	0	−100
P13	13	936	−74.46	762	−79.21
P27	27	1506	−58.91	1304	−64.42
P40	40	2101	−42.68	1842	−49.75
P53	53	2671	−27.14	2388	−34.86
P67	67	3212	−12.38	2855	−22.12
P80	80	3581	−2.31	3366	−8.18
P93	93	3665	−0.02	3655	−0.30
P30	100 (full)	3666	0	3666	0

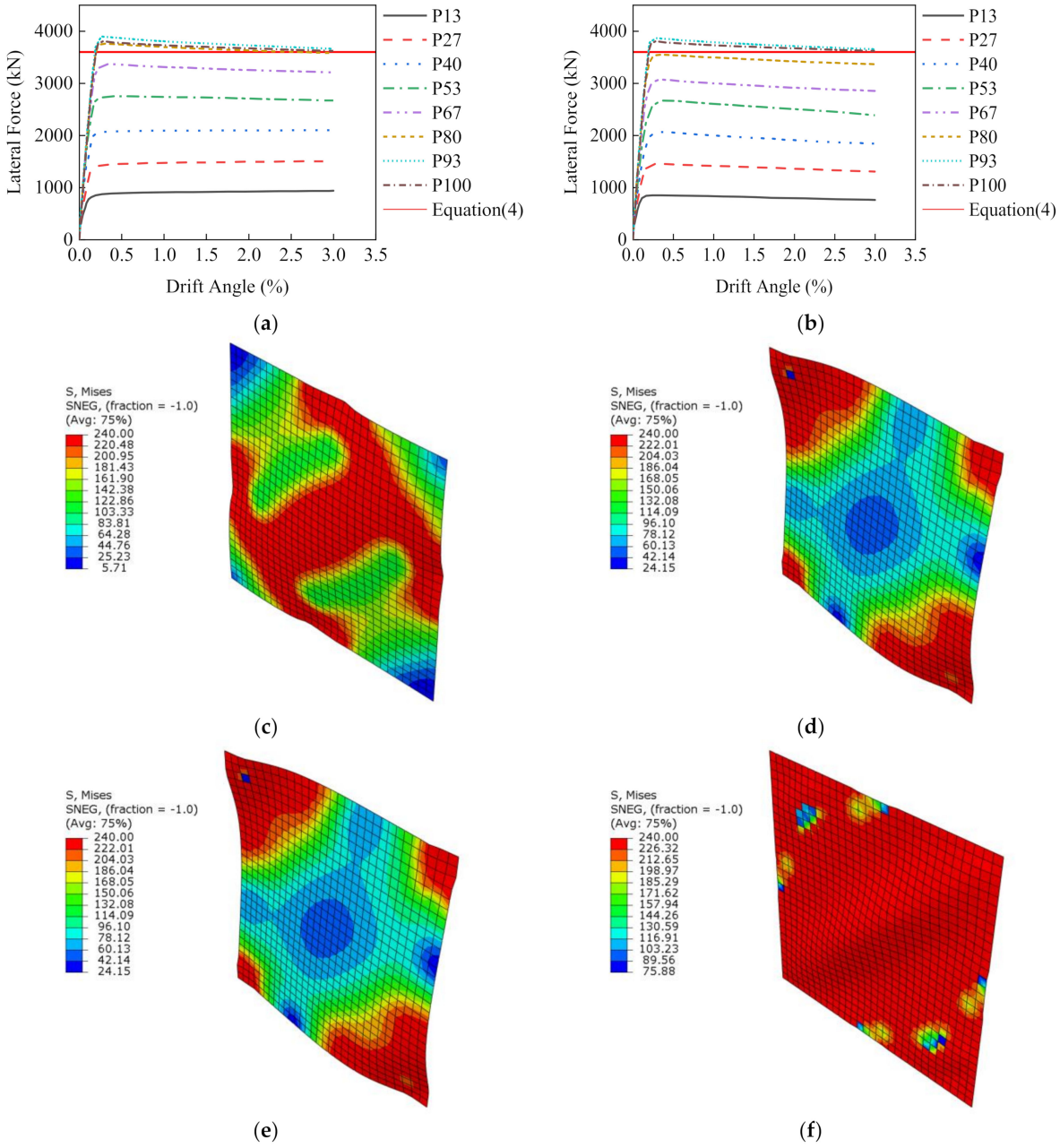


Figure 10. Load–displacement curves and stress distributions at 3% drift of S3 and S3R models: (**a**) S3; (**b**) S3R; (**c**) S3-P13; (**d**) S3R-P13; (**e**) S3-P80; (**f**) S3R-P80.

3.4. Structural Performance of S4 and S4R Models

S4 has a two-segment plate-to-frame connection, while S4R has a three-segment connection. Table 6 presents the shear strength of S4 and S4R. In Figure 11c, the S4-P20 has a large area yielding in the middle of the infill plate, whereas the corners are low stress or unstressed. In Figure 11d, the tension field exists on two sides of the S4R-P20 diagonal, yet the diagonal line does not yield. When the connectivity ratio of the S4-P80 and S4R-P80 is 80%, the shear strength is close to the full connection model. When the connection rate was 80% in Figure 11e,f, S4 and S4R almost fully yielded.

Table 6. Results of shear strength for S4 and S4R models.

Model	Connectivity Ratio γ (%)	S4		S4R	
		Value (kN)	Decrease Ratio (%)	Value (kN)	Decrease Ratio (%)
P0	Not connected	0	−100	0	−100
P20	20	1589	−56.65	1413	−61.45
P40	40	2463	−32.81	2238	−38.95
P60	60	3298	−10.03	3054	−16.69
P80	80	3638	−0.76	3587	−2.15
P100	100 (full)	3666	0	3666	0

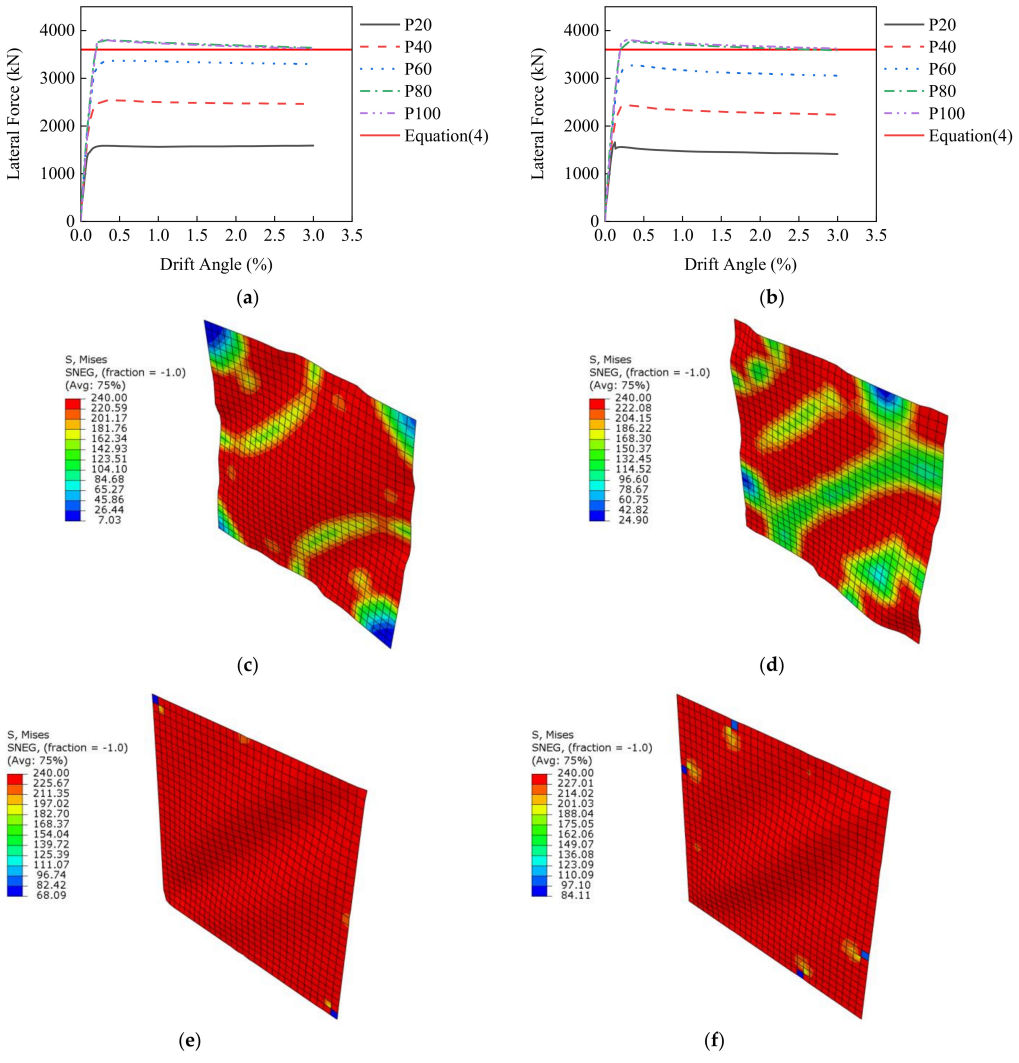


Figure 11. Load–displacement curves and stress distributions at 3% drift of S4 and S4R models: (**a**) S4; (**b**) S4R; (**c**) S4-P20; (**d**) S4R-P20; (**e**) S4-P80; (**f**) S4R-P80.

4. Discussion of Shear Strength of PC-SPSW

4.1. Influence of Partial Connection on Shear Strength

The shear capacities of partial connection steel plate shear walls are compared in Figure 12.

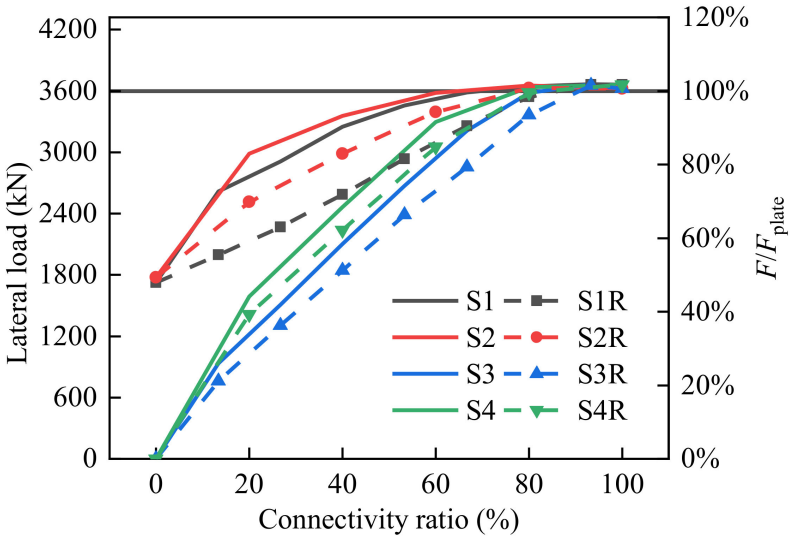


Figure 12. Relationship between shear strength and connectivity ratio.

Firstly, the effect of the connectivity ratio on the shear strength is examined. When the connectivity ratio is less than 50%, the shear strength of the fully beam-connected and partially column-connected types is greater than the four-edge partial connection because being fully beam-connected provides anchorage for the development of the infill plate tension field. Moreover, the low connectivity ratio prevents the infill plate from developing a significant area of the tension field, limiting the behavior of the infill plate material. The shear strength of the four-edge partial connection type increases with increasing the connectivity ratio. When the connectivity ratio hits 50%, even the shear strength of S4 exceeds that of S1R. Next, when the connectivity ratio exceeds 80%, the shear strength of both the two-edge partial connection and the four-edge partial connection is close to the case of the full connection. This is due to the infill plate's ability to produce a relatively complete tension field and fully develop the material properties of the steel plate.

Secondly, the influence of the connection types on the shear strength is analyzed. The fully beam-connected and partially column-connected types, such as S1 and S2, can still have approximately 80% of the shear strength even at the connectivity ratio of 20%. When the connectivity ratio is 60%, S1, S2, S2R, and S4 can retain more than 90% of the shear strength. Especially, S4 is partially connected on four edges, which means that the S4 model can utilize most of the material properties of the infill plate at a lower connectivity ratio. Therefore, the connection type of the S4 can significantly reduce the material and construction time required for plate-to-frame connection, and the S4 model is easy to construct and is a great connection type.

Next, the number of connected segments influences the shear strength. S1 and S3 are one-segment connections, while S2 and S4 are multi-segment connections. The shear strength of the steel plate shear wall with a multi-segment connection is higher than that of the one-segment connection for the same connectivity ratio. This is due to the fact that the multi-segment connection extends the connection range, making the area of the tension field more than that of the one-segment connection. Therefore, the distance of the segments can be selected appropriately.

Finally, the different effects of the connections from centers or corners on the shear strength are analyzed. For example, S1 and S3 are the connection from the centers, while S1R and S3R are the connection from the corners. Under the same connectivity ratio, the

shear strength of the connection from corners is basically lower than that from the centers. This is because the tension field is firstly generated along the diagonal when the infill plate buckles. The type of connection from the centers shows an obvious tension field in the diagonal direction, such as in Figure 10c. In the case of the connection from the corners, the tension field generated along the diagonal cannot develop effectively because there is no restraint in the middle of the infill plate. Therefore, most of the infill plate does not enter the yielding stage, and the shear strength of the structure is small (in Figure 10d). In summary, the influence of the central connection on the structural shear strength is higher than that of the corner connection.

4.2. Shear Strength Equations of S1 and S1R

The shear strength of the infill plate with different connectivity ratios is fitted according to the finite element model, as shown in Figure 13. The shear strength of the S1 model increases rapidly with increasing connectivity ratio when the connectivity ratio is low. By changing the width (b = 1500, 3000, 4500 mm) of the steel plate shear wall to change the width-to-height (aspect) ratio of the infill plate, the prediction Equation (10) still agrees well with the finite element results. The bearing capacity and the connectivity ratio of the S1R model can be simplified to a linear relationship. The prediction Equation (11) under different width-to-height ratios is also in good agreement with the finite element results. Equations (10) and (11) can accurately predict the shear strength. The parameter $h/(h + b)$ in Equations (10) and (11) can reflect the changes in the width-to-height (aspect) ratio of the infill plate. Furthermore, this parameter indicates the relationship between the length of partially connected models to the total length.

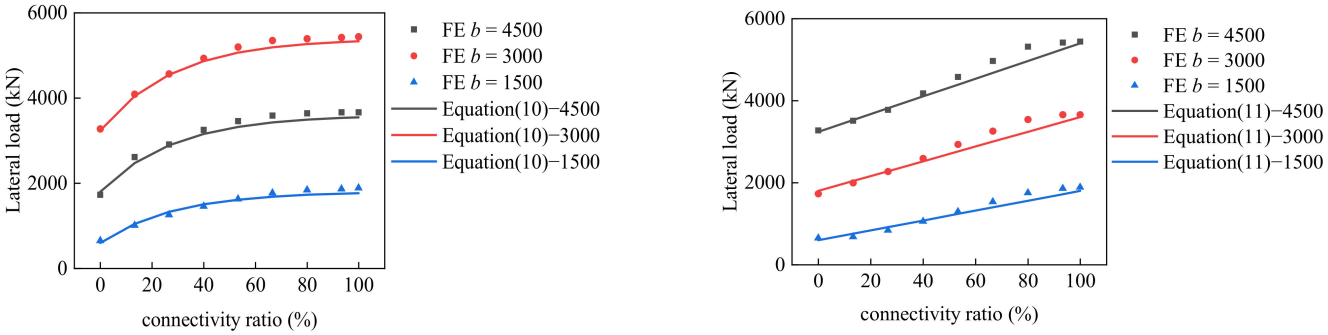


Figure 13. Comparison results of prediction equation and FE method for: (**a**) S1, and (**b**) S1R models.

When the plate is fully connected to the beams, the shear strength of the infill plate that is partially column-connected from the centers, such as S1, is shown in Equation (10). Equation (11) shows the shear strength of the infill plate that is partially column-connected from the corners, such as S1R.

$$F_{S1} = [1 - f_{S1}(\gamma)] \cdot F_{plate} = \left[1 - \frac{h}{h+b} e^{3.5\gamma}\right] \cdot \frac{1}{2} \sigma_y bt \sin(2\theta) \tag{10}$$

$$F_{S1R} = [1 - f_{S1R}(\gamma)] \cdot F_{plate} = \left[1 - \frac{h}{h+b}(1-\gamma)\right] \cdot \frac{1}{2} \sigma_y bt \sin(2\theta) \tag{11}$$

4.3. Shear Strength Equations of S2 and S2R

Figure 14 represents the relationship between shear strength and connectivity ratio for different width-to-height ratios of S2 and S2R. The predicted results from Equations (12) and (13) match the finite element values. The parameter $h/(h + b)$ reflects the changes in width-to-height ratios with the length of partially connected models.

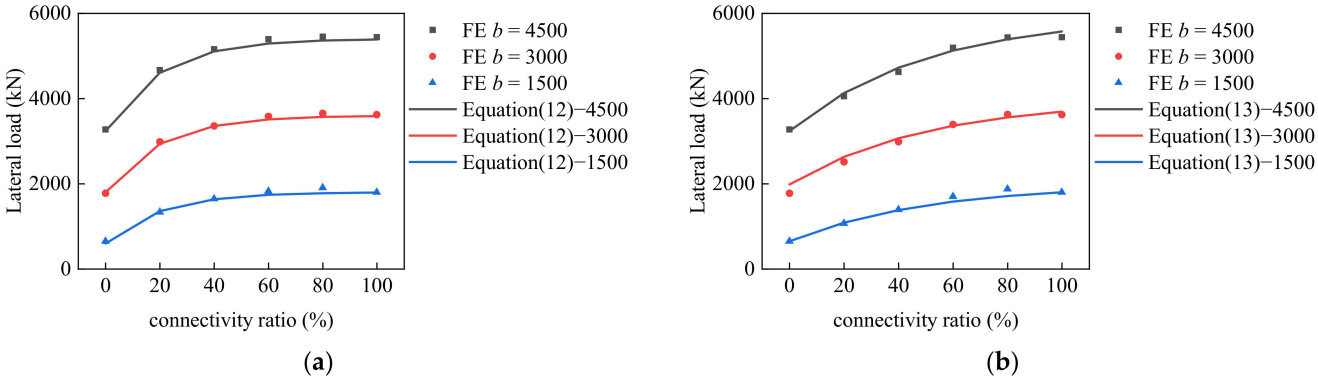


Figure 14. Comparison results of prediction equation and FE method for (**a**) S2 and (**b**) S2R models.

S2 and S1 are similar in connection types, therefore, Equation (12) is similar to Equation (10). However, the coefficients for the parameter of connectivity ratio are different. In the S2 example, the coefficient of the connectivity ratio is 5 in Equation (12), which is larger than the value of 3.5 in Equation (10). This coefficient reflects the influence of the number of connection segments on the shear strength. S1 is one segment connected, and S2 is two segments connected. The more segments, the greater the range of connection action.

$$F_{S2} = [1 - f_{S2}(\gamma)] \cdot F_{plate} = \left[1 - \frac{h}{h+b} e^{5\gamma}\right] \cdot \frac{1}{2} \sigma_y bt \sin(2\theta) \tag{12}$$

The equation for predicting the shear strength of the S2R type is shown as follows. In Equation (13), there is a constant of 1.1, which indicates the enhancement factor of the structure when the three segments of pate are connected from the centers and corners.

$$F_{S2R} = [1 - f_{S2R}(\gamma)] \cdot F_{plate} = \left[1.1 - \frac{h}{h+b} (1.1e^{\gamma})^2\right] \cdot \frac{1}{2} \sigma_y bt \sin(2\theta) \tag{13}$$

4.4. Shear Strength Equations of S3 and S4

The relationship between the shear strength and connectivity ratio of S3 and S4 is shown in Figure 15. Both S3 and S4 are the four-edged models partially connected to the beams and columns. Assuming the same connectivity ratio of beams and columns, here we only discuss the case of the width-to-height ratio of 1, that is, the parameter $(h + b)/(h + b)$ is 1. The prediction equations are consistent with the finite element results. The connection type of S3 is similar to S1, but the difference is that they are two-edge or four-edge partial connection models. Comparing Equations (14) and (10), the coefficient for the parameter of connectivity ratio is reduced by half to be 1.75, and the enhancement factor is 1.2. Similar conclusions can be drawn from Equations (15) and (12) for S4 and S2, where the coefficient for the parameter of connectivity ratio is also reduced by half to be 2.5 and the enhancement factor is 1.1.

$$F_{S3} = [1 - f_{S3}(\gamma)] \cdot F_{plate} = \left[1.2\left(1 - \frac{h+b}{h+b} e^{1.75\gamma}\right)\right] \cdot \frac{1}{2} \sigma_y bt \sin(2\theta) \tag{14}$$

$$F_{S4} = [1 - f_{S4}(\gamma)] \cdot F_{plate} = \left[1.1\left(1 - \frac{h+b}{h+b} e^{2.5\gamma}\right)\right] \cdot \frac{1}{2} \sigma_y bt \sin(2\theta) \tag{15}$$

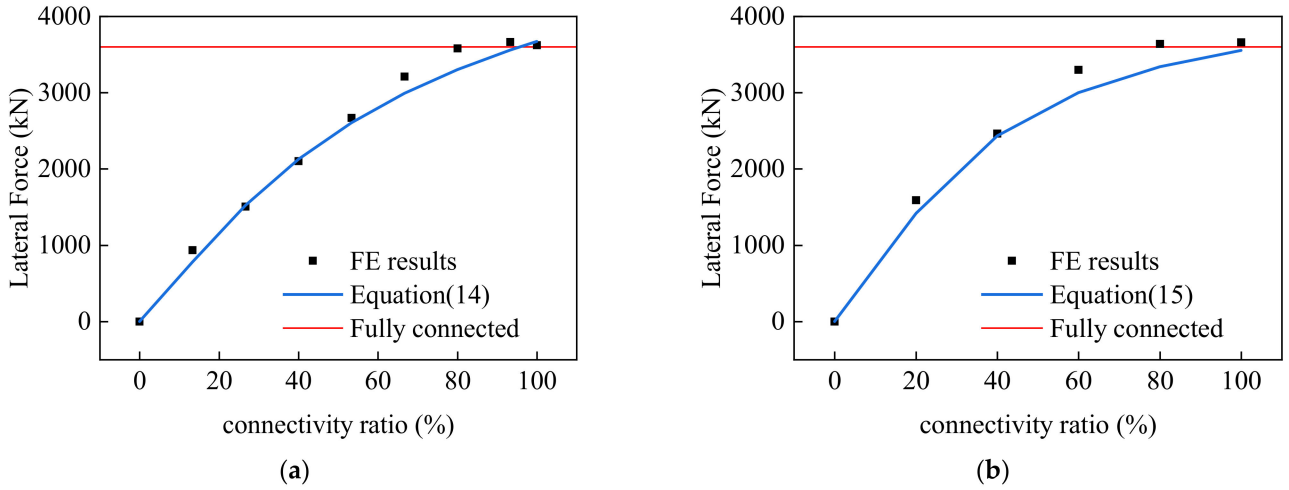


Figure 15. Comparison results of prediction equation and FE method for: (**a**) S3, and (**b**) S4 models.

5. Conclusions

1. This research proposes eight different types of plate-to-frame connections and investigates the effect of the connectivity ratio on the shear strength of the steel plate shear wall. When the infill plate is only connected to beams, the shear strength decreases by nearly 50% compared to the full connection. However, when the central part of the plate is connected to the column, such as S1 and S2, the load-bearing capacity of the structure is significantly higher than that of the beam-only connection. When the connectivity ratio of plate-to-columns hits 67%, the shear strength of the structure is almost equivalent to the full connection.
2. Considering the connectivity ratio and width-to-height ratio, the formulae of shear strength with different connection types are presented. The prediction formula correlates with the finite element results well. The shear strength increases rapidly with an increase in the connectivity ratio. When the connection ratio reaches 80%, the shear strength of the structure reaches more than 95% of the full connection type.
3. Multi-segment connections obtain a higher shear strength than one-segment connections at the same connectivity ratio. Increasing the connectivity ratio of the plate from the centers can improve the shear strength of the structure more than from the corners.

Author Contributions: Conceptualization, Y.Y. and Z.M.; methodology, Y.Y.; software, Y.Y.; validation, Y.Y.; formal analysis, Y.Y.; investigation, Y.Y.; resources, Y.Y., Z.M. and B.Z.; data curation, Y.Y.; writing—original draft preparation, Y.Y.; writing—review and editing, Z.M. and B.Z.; visualization, Y.Y.; supervision, Z.M. and B.Z.; project administration, Z.M.; funding acquisition, Z.M. All authors have read and agreed to the published version of the manuscript.

Funding: This research was funded by the National Natural Science Foundation of China, grant number 51578064 and the Natural Science Foundation of Beijing Municipality grant number 8172031.

Institutional Review Board Statement: Not applicable.

Informed Consent Statement: Not applicable.

Data Availability Statement: All the data supporting the results were provided within the article.

Conflicts of Interest: The authors declare no conflict of interest.

References

1. Elgaaly, M. Thin steel plate shear walls behavior and analysis. *Thin-Walled Struct.* **1998**, *32*, 151–180. [CrossRef]
2. Wagner, H. *Flat Sheet Metal Girder with Very Thin Metal Web: Part I General Theories and Assumptions*; Technical Memorandum, No. 604; National Advisory Committee for Aeronautics: Moffett Field, CA, USA, 1931.
3. Basler, K. Strength of plate girders in shear. *J. Struct. Div. ASCE* **1961**, *87*, 151–180. [CrossRef]

4. Thorburn, L.J.; Kulak, G.L.; Montgomery, C.J. *Analysis of Steel Plate Shear Walls*; Structural Engineering Report. No. 107; Department of Civil Engineering, University of Alberta: Edmonton, AB, Canada, 1983.
5. Jin, S.; Yang, S.; Bai, J. Numerical and experimental investigation of the full-scale buckling-restrained steel plate shear wall with inclined slots. *Thin-Walled Struct.* **2019**, *144*, 106362. [CrossRef]
6. Mu, Z.; Yang, Y. Experimental and numerical study on seismic behavior of obliquely stiffened steel plate shear walls with openings. *Thin-Walled Struct.* **2020**, *146*, 106457. [CrossRef]
7. Farahbakhshtooli, A.; Bhowmick, A.K. Nonlinear seismic analysis of perforated steel plate shear walls using a macro-model. *Thin-Walled Struct.* **2021**, *166*, 108022. [CrossRef]
8. Tong, J.; Guo, Y.; Zuo, J.; Gao, J. Experimental and numerical study on shear resistant behavior of double-corrugated-plate shear walls. *Thin-Walled Struct.* **2020**, *147*, 106485. [CrossRef]
9. Azandariani, M.G.; Gholhaki, M.; Kafi, M.A. Experimental and numerical investigation of low-yield-strength (LYS) steel plate shear walls under cyclic loading. *Eng. Struct.* **2020**, *203*, 109866. [CrossRef]
10. De Matteis, G.; Brando, G.; D'Agostino, M.F.M. Experimental analysis of partially buckling inhibited pure aluminium shear panels. In *Behaviour of Steel Structures in Seismic Areas*; CRC Press: Boca Raton, FL, USA, 2012; pp. 809–814. [CrossRef]
11. De Matteis, G.; Brando, G. Comparative analysis of dual steel frames with dissipative metal shear panels. *Key Eng. Mat.* **2018**, *763*, 735–742. [CrossRef]
12. Yu, J.; Huang, J.; Li, B.; Feng, X. Experimental study on steel plate shear walls with novel plate-frame connection. *J. Constr. Steel Res.* **2021**, *180*, 106601. [CrossRef]
13. Paslar, N.; Farzampour, A.; Hatami, F. Infill plate interconnection effects on the structural behavior of steel plate shear walls. *Thin-Walled Struct.* **2020**, *149*, 106621. [CrossRef]
14. Azandariani, G.M.; Rousta, A.M.; Mohammadi, M.; Rashidi, M.; Abdolmaleki, H. Numerical and analytical study of ultimate capacity of steel plate shear walls with partial plate-column connection (SPSW-PC). *Structures* **2021**, *33*, 3066–3080. [CrossRef]
15. Wei, M.; Liew, J.Y.R.; Fu, X. Panel action of novel partially connected buckling-restrained steel plate shear walls. *J. Constr. Steel Res.* **2017**, *128*, 483–497. [CrossRef]
16. Wei, M.; Liew, J.Y.R.; Yong, D.; Fu, X. Experimental and numerical investigation of novel partially connected steel plate shear walls. *J. Constr. Steel Res.* **2017**, *132*, 1–15. [CrossRef]
17. Du, Y.; Zhang, Y.; Zhou, T.; Chen, Z.; Zheng, Z.; Wang, X. Experimental and numerical study on seismic behavior of SCFRT column frame-buckling restrained steel plate shear wall structure with different connection forms. *Eng. Struct.* **2021**, *239*, 112355. [CrossRef]
18. Mirsadeghi, H.M.R.; Fanaie, N. Steel plate shear walls with partial length connection to vertical boundary element. *Structures* **2021**, *32*, 1820–1838. [CrossRef]
19. ABAQUS. *Analysis User's Manual IV. Version 6.10*; ABAQUS, Inc.: Palo Alto, CA, USA; Dassault Systèmes: Vélizy-Villacoublay, France, 2010.
20. Asl, M.H.; Safarkhani, M. Seismic behavior of steel plate shear wall with reduced boundary beam section. *Thin-Walled Struct.* **2017**, *116*, 169–179. [CrossRef]
21. Machaly, E.B.; Safar, S.S.; Amer, M.A. Numerical investigation on ultimate shear strength of steel plate shear walls. *Thin-Walled Struct.* **2014**, *84*, 78–90. [CrossRef]
22. Wang, M.; Zhang, X.; Yang, L.; Yang, W. Cyclic performance for low-yield point steel plate shear walls with diagonal T-shaped-stiffener. *J. Constr. Steel Res.* **2020**, *171*, 106163. [CrossRef]
23. Shekastehband, B.; Azaraxsh, A.A.; Showkati, H.; Pavir, A. Behavior of semi-supported steel shear walls: Experimental and numerical simulations. *Eng. Struct.* **2017**, *135*, 161–176. [CrossRef]
24. Sigariyazd, M.A.; Joghataie, A.; Attari, N.K.A. Analysis and design recommendations for diagonally stiffened steel plate shear walls. *Thin-Walled Struct.* **2016**, *103*, 72–80. [CrossRef]
25. Timoshenko, S.P.; Gere, J.M. *Theory of Elastic Stability*; McGraw-Hill Publishing Company: New York, NY, USA, 1961.
26. Sabelli, R.; Bruneau, M. *Steel Design Guide of Steel Plate Shear Walls*; No. 20; American Institute of Steel Construction (AISC): Chicago, IL, USA, 2007.
27. Ozcelik, Y.; Clayton, P.M. Strip model for steel plate shear walls with beam-connected web plates. *Eng. Struct.* **2017**, *136*, 369–379. [CrossRef]
28. Nascimbene, R. Towards Non–standard numerical modeling of thin-shell structures: Geometrically linear formulation. *Int. J. Comput. Methods Eng. Sci. Mech.* **2014**, *15*, 126–141. [CrossRef]
29. *BS-EN 1993-1-6:2007*; Eurocode 3: Design of Steel Structures Part 1–6: Strength and Stability of Shell. European Committee for Standardization: Brussels, Belgium, 2007.
30. Habashi, H.R.; Alinia, M.M. Characteristics of the wall–frame interaction in steel plate shear walls. *J. Constr. Steel Res.* **2010**, *66*, 150–158. [CrossRef]